Field–free molecular alignment of CO2 mixtures in presence of collisional relaxation

5 AUTHORS, INCLUDING:

Thomas Vieillard
8 PUBLICATIONS   189 CITATIONS

SEE PROFILE

Frederic Chaussard
Laboratoire Interdisciplinaire Carnot de Bo…
32 PUBLICATIONS   315 CITATIONS

SEE PROFILE

Dominique Sugny
University of Burgundy
131 PUBLICATIONS   1,451 CITATIONS

SEE PROFILE

B. Lavorel
University of Burgundy
174 PUBLICATIONS   2,859 CITATIONS

SEE PROFILE

JRS

Field-free molecular alignment of CO₂ mixtures in presence of collisional relaxation

T. Vieillard, F. Chaussard,* **D. Sugny, B. Lavorel and O. Faucher**

Institut Carnot de Bourgogne, UMR CNRS 5209, Département OMR, Université de Bourgogne 9 avenue Alain Savary BP 47870 21078 Dijon, Cedex, France

The present work explores the extension of the concept of short-pulse-induced alignment to dissipative environments within quantum mechanical density matrix formalism (Liouville equation) from the weak to the strong field regime. This is illustrated within the example of the CO₂ molecule in mixture with Ar and He, at room temperature, for which a steep decrease of the alignment is observed at moderate pressure because of the collisional relaxation. The field-free alignment is measured by a polarization technique where the degree of alignment is monitored in the time domain by measuring the resulting transient birefringence with a probe pulse Raman induced polarization spectroscopy (RIPS) Copyright © 2008 John Wiley & Sons, Ltd.

INTRODUCTION

Alignment and orientation of molecules are of great importance for chemical reaction dynamics, molecular optics, nonlinear optics and strong field molecular physics (for a recent review see Refs 1, 2). In a nonadiabatic regime, when the pulse duration is much shorter than the rotational period of the molecule (typically a few ps to tens of ps), periodic alignment corresponding to a rephasing of the rotational wavepacket created by the pump pulse, as well as planar delocalization take place in a field-free condition.[2–5] Moreover, in the nonperturbative regime of intensity, high J-states can be excited, but the M quantum number being conserved during the interaction, molecules can have a rotational angular momentum J larger than their projection along the polarization axis, leading to a permanent postpulse alignment. Such a molecular field-free alignment has now been quite widely observed by several groups but those studies have focused either on 'isolated' molecules (cold molecular beam experiments) or low-density media (few tens or hundreds of millibars).[1,6,7] Though, there are a real fundamental interest and practical potential of alignment in a dissipative medium, may it be a dense gas or a liquid. Recently, the concept of nonadiabatic alignment has been extended to the dissipative media limit, within a density matrix approach, but only from a theoretical point

of view.[8–11] The authors illustrated the possibility through such studies to get independent informations about the rotational population relaxation and the pure phase-decoherence effects. To our knowledge, no experimental works in dissipative environments have been reported so far.

The goal of the present work is to present a first preliminary comparison between the theoretical approach mentioned above and experimental results, in the case of CO₂ molecules self-perturbed and in Ar and He gas, in a wide intensity range.

THEORY

In the following, we will focus our attention to the CO₂ linear molecule interacting with a linearly polarized, nonresonant laser pulse.[6] The most relevant, and thus common observable of the time dependent alignment of the molecule is given by $\cos^2\theta$ where θ is the angle between the molecular axis and the polarization direction of the laser field. The experiment allows us to measure the expectation value $\langle\cos^2\theta\rangle$. In order to describe the influence of the surrounding environment, it is straightforward to use the framework of the density operator, the expectation value $\langle\cos^2\theta\rangle$ being given by $Tr(\cos^2\theta\rho(t))$. $\rho(t)$ is the density operator and is expanded in terms of the rigid rotor eigenstates $|J'M'\rangle$.[8–10,12] Its time evolution is assumed to obey the Redfield Eqn,[13] as follows:

$$\frac{d\rho(t)}{dt} = -\frac{i}{\hbar}[H_0, \rho(t)] + \Omega(t)[V, \rho(t)] + \left(\frac{d\rho(t)}{dt}\right)_{\text{diss}} \quad (1)$$

*Correspondence to: F. Chaussard, Institut Carnot de Bourgogne, UMR CNRS 5209, Département OMR, Université de Bourgogne 9 avenue Alain Savary BP 47870 21078 Dijon, Cedex, France.
E-mail: frederic.chaussard@u-bourgogne.fr

where, in the case of the alignment process,

$$H_0 = BJ^2 - DJ^4 \qquad (2)$$

$$V = \cos^2\theta \qquad (3)$$

$$\Omega(t) = -\frac{1}{4}\mathcal{E}^2(t)\Delta\alpha \qquad (4)$$

where J stands for the angular momentum operator, B is the rotational constant, D the centrifugal distortion, $\Delta\alpha = \alpha_{//} - \alpha_{\perp}$ the difference between the parallel and perpendicular components of the polarizability tensor. $\mathcal{E}(t)$ is the envelope of the laser electric field which has been assumed to be Gaussian in our case: $\mathcal{E}(t) = \mathcal{E}_0\exp\left(-\frac{2\sqrt{\ln 2}t}{\tau_p}\right)^2$ with $\mathcal{E}_0$ the peak amplitude and τ_p the full width at half-maximum (FWHM).

The last term of Eqn (1) describes the rotational relaxation processes due to elastic and inelastic collisions between CO₂ molecules and perturbers (CO₂ itself, *Ar* or *He* in our case). Within the framework mentioned above, this dissipative dynamics can be described by means of the so-called relaxation matrix (which elements $K_{JMJ'M'}$ are the rates of population transfer from state to state $|JM\rangle$ to state $|J'M'\rangle$), and by an extra term, denoted as $\gamma^{(pd)}_{JMJ'M'}$ representing the pure decoherence rate of phase between state $|JM\rangle$ and state $|J'M'\rangle$. Here, decoherence has to be understood as loss of phase. In order to evidence the contribution of each relaxation process, the time evolution of the dissipative term can be split in two sets of coupled differential equations, as below, for off-diagonal and diagonal elements, respectively tied to the elastic relaxations (i.e. pure dephasing), and to the relaxation through inelastic collisions (i.e. population transfert):

$$\left(\frac{d\rho_{JMJ'M}(t)}{dt}\right)_{diss}$$
$$= -\frac{1}{2}\sum_{J_1,M_1}[K_{JMJ_1M_1} + K_{J'MJ_1M_1}]\rho_{JMJ'M}(t) - \gamma^{(pd)}_{JMJ'M}\rho_{JMJ'M}(t)$$
$$(5)$$

$$\left(\frac{d\rho_{JMJM}(t)}{dt}\right)_{diss}$$
$$= -\sum_{J_1,M_1}[K_{JMJ_1M_1}\rho_{JMJM}(t) - K_{J_1M_1JM}\rho_{J_1M_1J_1M_1}(t)] \qquad (6)$$

wherein, we assume that the quantum number M is conserved (selection rules for a linear polarization of the pump field). The coefficients $K_{JMJ'M'}$ are the rates of population transfer from state $|JM\rangle$ to state $|J'M'\rangle$. They are described by means of empirical scaling laws. In the present work, we use energy-corrected sudden (ECS) laws, namely ECS-P when the perturber is CO₂ itself or Helium and ECS-EP when the perturber is Argon. The rates of population are thus given by[12,14]

$$K_{JJ'} = A(T_0)\left(\frac{T}{T_0}\right)^{-N}(2J'+1)\exp\left(\frac{(E_J - E_{J>})}{k_BT}\right)$$

$$\times\sum_L\left\{\begin{pmatrix}J & J' & L\\0 & 0 & 0\end{pmatrix}^2\frac{2L+1}{(L(L+1))^\alpha}\left(\frac{1+\omega^2_{L,L-2}\tau_c^2/24}{1+\omega^2_{J,J-2}\tau_c^2/24}\right)^2\right.$$
$$\left.\exp\left(-\beta\frac{E_L}{k_BT}\right)\right\} \qquad (7)$$

with $J \geq max(J,J')$, $\omega_{J,J-2} = (E_J - E_{J-2})/\hbar$ and $\tau_c = l_c/\overline{v}$ ($\overline{v} = \sqrt{8k_bT/\pi\mu}$ and μ the reduced mass). The set of parameters is given by Table 1.[15]

In this work $T_0 = 300$ K. N is known for CO₂ and take the value $N = 0.97$ but it is unknown for Ar and He as perturbers. Nevertheless, as T = 295 K the ratio T/T_0 is about 1 and so the determination of N for this two molecules is not required.

To date, no data on the pure phase decoherence term $\gamma^{(pd)}_{JMJ'M'}$ are available but experimental results allow us to think that it is negligible within the framework of our work, i.e at pressure below 2 bars.[12]

As said above, the observable which describes the alignment is $\langle\cos^2\theta\rangle$. The decomposition of the Liouville equation into diagonal and off-diagonal terms leads us to recast $\langle\cos^2\theta\rangle$ as

$$\langle\cos^2\theta\rangle = \langle\cos^2\theta\rangle_p + \langle\cos^2\theta\rangle_c \qquad (8)$$

where $\langle\cos^2\theta\rangle_p$ gives the time evolution of alignment due to the population of rotational states (permanent alignment) and $\langle\cos^2\theta\rangle_c$ give the time evolution of alignment due to coherence (transient alignment). In terms of the density matrix elements, those two quantities are given by:

$$\langle\cos^2\theta\rangle_p = \sum_{J,M}\rho_{JMJM}(t)V_{JMJM} \qquad (9)$$

$$\langle\cos^2\theta\rangle_c = \sum_{J\neq J',M}\rho_{JMJ'M}(t)V_{JMJ'M} \qquad (10)$$

At the thermal equilibrium (when the medium is isotropic) Eqn (9) takes the value $1/3$ and Eqn (10) equals to 0. After the interaction with the laser pulse, a superposition of rotational levels is created and $\langle\cos^2\theta\rangle_p$ may reach a value greater than $1/3$ which depends on the laser intensity and which tends toward $1/2$. This value can be interpreted as a permanent alignment. In the absence of a dissipative environment, this permanent alignment would remain indefinitely. However, when collisional processes occur, $\langle\cos^2\theta\rangle_p$ decreases more or less slowly down to its thermal equilibrium value. The rate of this decrease is

Table 1. Parameters for Eqn (7)

	CO₂–CO₂	CO₂–Ar	CO₂–He
A (10^{-3} cm¹.atm⁻¹)	45	18.1	35.2
l_c (Å)	1.4	3.43	0.54
β	0 (ECS-P)	0.02	0 (ECS-P)
α	0.94	0.818	1.014

directly connected to the *K* coefficients, and concomitantly to the density of the medium. Meanwhile, the laser excitation also creates coherences in the system: this corresponds to a nonzero value of $\langle\cos^2\theta\rangle_c$ which oscillates at the rotational period. Owing to decoherence, the amplitude of these rotational revivals decay toward its equilibrium value.

EXPERIMENTAL

The time evolution of the alignment of the CO_2 molecule is measured by means of a Raman induced polarization spectroscopy (RIPS) experiment. This method is based upon the modification of the polarization of a probe beam by the studied medium.[16,17] The technique thus relies on a birefringence measurement. The expression of the signal is given by

$$I_{RIPS}(\tau) \propto [(\langle\cos^2\theta\rangle(t) - 1/3)^2 \otimes \mathcal{E}^2_{probe}(t)]_{t=\tau} \qquad (11)$$

It is noteworthy that this pump–probe setup leads to a measure which is directly related to the degree of alignment.

Although already described elsewhere, the setup, whose scheme is shown in Fig. 1, is briefly recalled here. The laser source consists of a chirped, pulsed, amplified Ti : sapphire femtosecond laser operating at a 1 kHz repetition rate and delivering pulses with 90–100 fs duration and a spectrum centered at 800 nm. The initial output beam is split into

two parts (pump and probe beam, both linearly polarized at 45° with respect to each other), separated by a temporal delay adjusted by a corner tube reflector mounted on a motorized linear stage. The pump and probe beams are focused by a focal length lens and crossed at a small angle in the studied gas. The depolarization of the probe beam (i.e. the expected birefringence signal) is measured thanks to an analyzer whose neutral axis is perpendicular to the initial polarization axis of the probe and collected by a photomultiplier sampled by a boxcar integrator.

All the experiments were carried out at room temperature, in a static cell. The intensities and pressures used for the three mixtures are recalled in Table 2.

The concentration of the mixtures is 90% of Ar or He and 10% of CO_2. Figure 2 represents a typical RIPS signal in pure CO_2. In the following, we will particularly be interested in the evolution of the first, third, fourth and ninth transients, framed on Fig. 2.

Table 2. Intensities and pressures used for mixtures

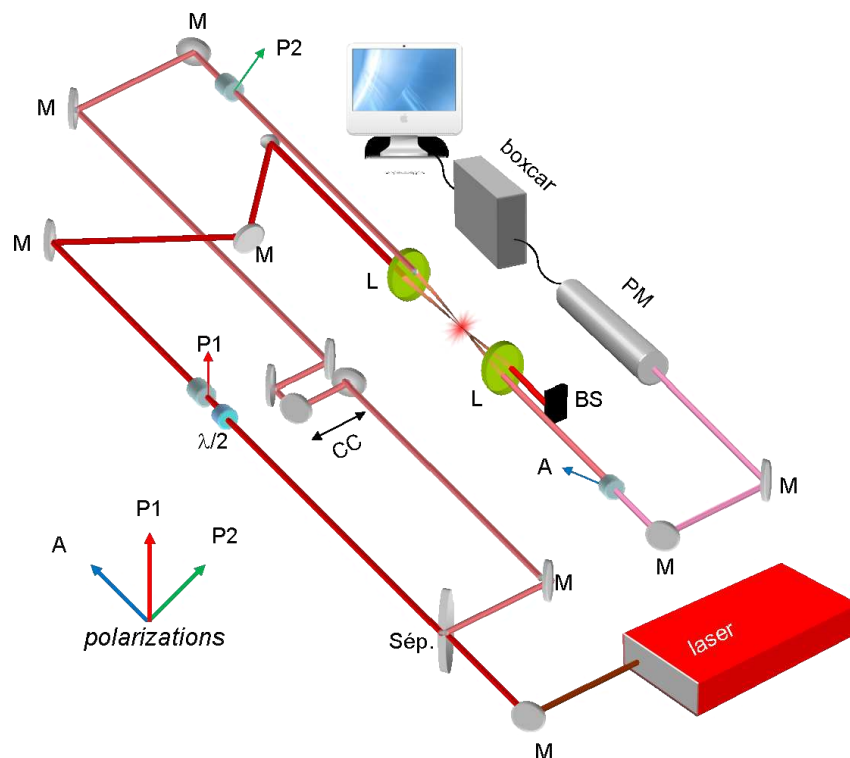| Mixture	Min/max I_{exp} (TW/cm²)	pressure (bar)
CO_2	20/217	1
CO_2–Ar	20/100	1.1
CO_2–He	20/100	1

Figure 1. Experimental setup: M, mirror; Sép, beam Splitter; CC, cube corner; L, lens; BS, beam stop; PM, photomultiplier. The relative polarizations of the various polarizers are called back at the bottom left. This figure is available in colour online at www.interscience.wiley.com/journal/jrs.
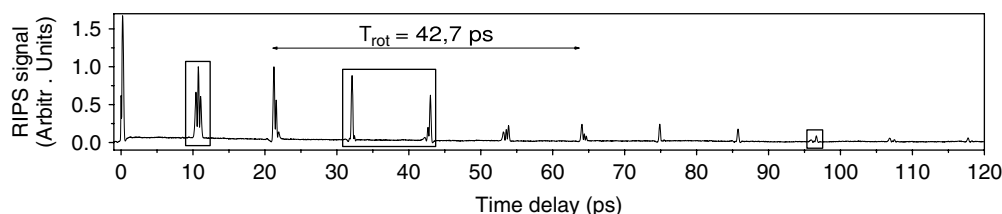
Figure 2. Typical RIPS signal for pure CO$_2$ at T = 295 K, P = 1 bar and $I_{peak}^{exp} = 128$ TW/cm^2.
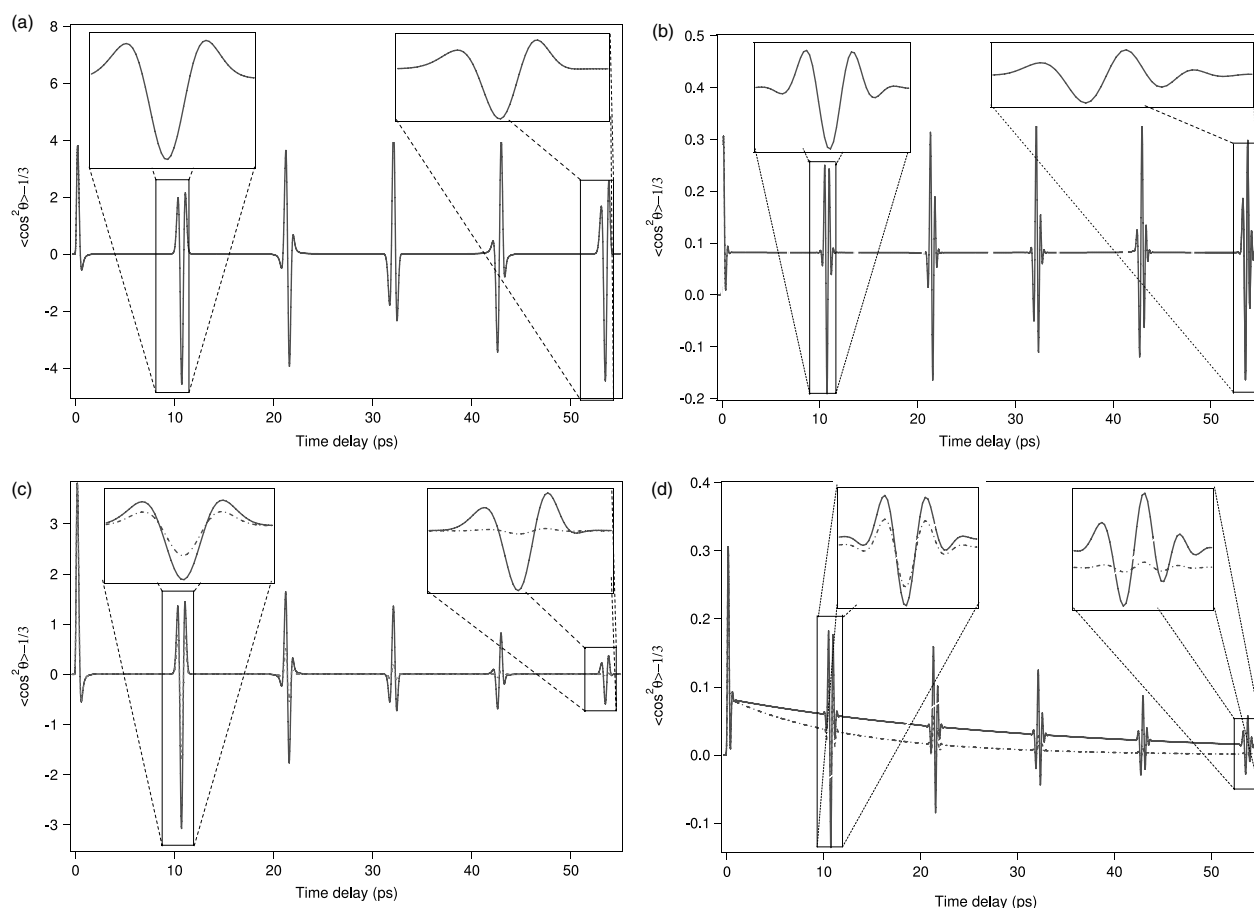

Figure 3. Simulation of $\langle \cos^2 \theta \rangle - 1/3$ with (c, d) and without (a, b) dissipation. (c) and (d) present a simulation for P = 2 bar (full line) and P = 5 bar (dash line). (a) and (c) are calculated with a weak field ($I_{peak} = 1$ TW/cm^2). (b) and (d) are calculated with a strong field ($I_{peak} = 100$ TW/cm^2).

SIMULATIONS

In this section, we propose to qualitatively discuss the time evolution of $\langle \cos^2 \theta \rangle - 1/3$ vs the intensity regime in the presence or in the absence of relaxation processes. The different panels in Fig. (3) display the case of the weak field limit ($I_{peak} = 1$ TW/cm^2, Figure 3(a), 3(c)) and the strong one ($I_{peak} = 100$ TW/cm^2, 3b,3d).

We notice the well-known revival structures equally spaced by a quarter of the rotational period. These structures are described by the $\langle \cos^2 \theta \rangle_c$ term introduced in a previous section. During each transient, a positive value of

$\langle \cos^2 \theta \rangle - 1/3$ is associated with an alignment of the molecular axis along the field axis, whereas a negative value is linked to a planar delocalization of the molecular axis in the equatorial plane. It directly measures the time evolution of the coherence.

In the weak field limit Fig. 3(a), a zero background value is observed between two recurrences, meaning that the medium goes back to an isotropic situation. It is no longer the case when increasing the pump field strength, i.e. the intensity Fig. 3(b). A significant nonzero value is then obtained, and is interpreted as a permanent alignment, coming from the contribution to the rotational wavepacket

of eigenstates with $\bar{J} \geq M$ where $\bar{J}$ is the average value of the populated states and M the magnetic quantum number. It corresponds to the $\langle \cos^2 \theta \rangle_p$ term. The degree of this permanent alignment is directly related to the intensity and when no dissipation is introduced, it never dies out and keeps its initial amplitude. When the intensity grows, one can also notice a shape change of the transients: as higher J-states being populated, the distribution of the wavepacket in the J-space is broadened, and thus leads to narrower transients, as observed in Fig. 3(b).

In the dissipative case (i.e. here, when the gas pressure is increasing. Figures 3(c), 3(d)) both components exhibit a monotonic decay down to their equilibrium values due to elastic collisions for $\langle \cos^2 \theta \rangle_c$ and inelastic ones (J-changing) for $\langle \cos^2 \theta \rangle_p$.

It is noteworthy that, when the pure decoherence term $\gamma_{JMJ'M'}^{(pd)}$ is zero, $\langle \cos^2 \theta \rangle_c$ and $\langle \cos^2 \theta \rangle_p$ decay with the same rate. That is the case in the gas phase, for which this pure decoherence term has been often found negligible, at least at moderate pressures. The situation would be somewhat different in the liquid phase where it would have a significant effect.

The important thing to point out is that through a numerical simulation fitted to experiment and the decomposition of the alignment observable $\langle \cos^2 \theta \rangle$ in terms of $\langle \cos^2 \theta \rangle_p$ and $\langle \cos^2 \theta \rangle_c$, it is possible to directly access to the pure phase decoherence and population relaxation mechanisms which usually remain entangled when measured in the frequency domain.

RESULTS AND DISCUSSION

The model described in the theoretical part is used to perform numerical simulations which are fitted to the experimental data. Two parameters are let free for this numerical adjustment: a scaling factor and the pump intensity. It must be noticed here that this intensity represents an effective intensity, inasmuch as the volume effects[18] and the spatial distribution of the laser beam are not included in the model.

Figure 4 presents the experimental evolution vs intensity of transient alignments and the corresponding simulations for CO_2 and CO_2–Ar mixture. On first transients we observe that the relative height of the central peak (peak of delocalization), compared to the amplitudes of the two side peaks, tends to decrease when the intensity of the pump increases. The width of the two calculated side peaks decreases when the intensity increases, leading to a reduction in the total width of the transient. The same behavior can be observed on the third and fourth transients.

Whereas the calculation reproduced quite well the experimental signal up to the third transient whatever be the intensity; a slight discrepancy appears when looking at the fourth transient. Then, the agreement between experimental and calculated get worse at further delays, the former
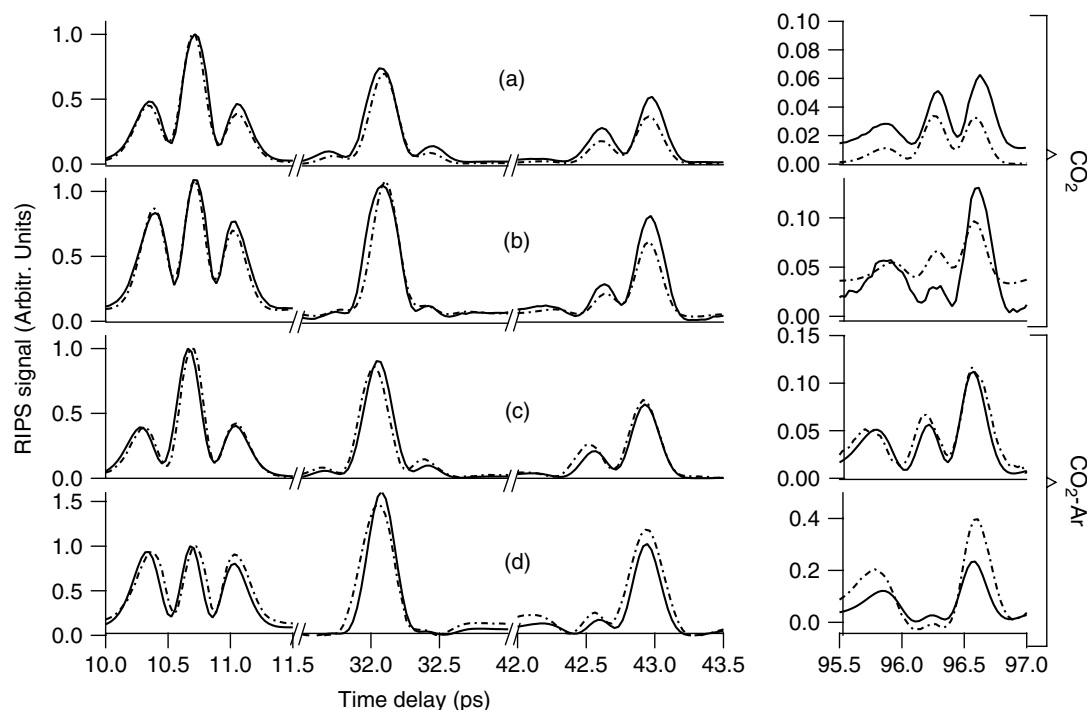

Figure 4. Evolution of alignment transients of pure CO_2 [(a) and (b)) and of CO_2–Ar mixture ((c) and (d)] according to pump field intensity. Full lines correspond to experimental data and dashed line to simulated data. Part (a) corresponds to $I_{peak}^{exp} = 51\ TW/cm^2$ ($I_{peak}^{sim} = 59\ TW/cm^2$), (b) corresponds to $I_{peak}^{exp} = 217\ TW/cm^2$ ($I_{peak}^{sim} = 102\ TW/cm^2$), (c) corresponds to $I_{peak}^{exp} = 20\ TW/cm^2$ ($I_{peak}^{sim} = 17\ TW/cm^2$) and (d) corresponds to $I_{peak}^{exp} = 100\ TW/cm^2$ ($I_{peak}^{sim} = 70\ TW/cm^2$).
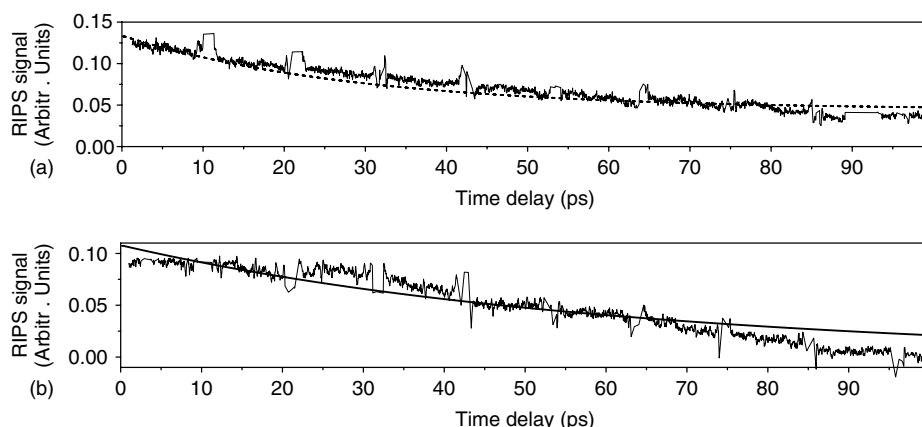
Figure 5. Evolution of permanent alignment of pure CO_2 (a) and of CO_2–Ar. Full lines correspond to experimental data and dashed lines correspond to simulated data. Part (a) corresponds to $I_{peak}^{exp} = 217\ TW/cm^2$ ($I_{peak}^{sim} = 102\ TW/cm^2$) and (b) corresponds to $I_{peak} = 100\ TW/cm^2$ ($I_{peak}^{sim} = 70\ TW/cm^2$).

exhibiting slower decays than the latter. The decay rate depends on the K coefficient values; other laws different from the ECS law have been tested (such as modified exponential gap laws (MEG)[19]), but they all lead to identical results.

We now analyze the specific evolution of the permanent alignment. Figure 5 displays the base line of experimental signals for pure CO_2 and CO_2–Ar. Contrary to the observations made above for the amplitudes of the transients, the permanent alignment dynamics seems to be quite correctly reproduced by the model. The same agreement has been also observed in the case of CO_2–He mixture. One must recall that the decay of the permanent alignment is tied to the population relaxation, i.e. the diagonal elements of the density matrix, whereas coherences are described by the off-diagonal terms. The observed discrepancy may thus come from the modelization of the latter ones, but no explanation has been found so far.

CONCLUSION

The present study constitutes a very first attempt to compare field-free molecular alignment experiments not restricted to a low-density regime and a theoretical model based on a density matrix formalism. Though limited to the case of CO_2 (self-perturbed or with perturbers such as argon or helium) at moderate pressures, the performed experiments are at least qualitatively reproduced by the simulations which give the correct transient shapes. However, except for the very short delay transients, a discrepancy is observed for all the mixtures as for the amplitudes and thus the decay rates for transient alignments, whereas the decay of the permanent alignment is quite well described. Possible explanations could come from the modelization of the off-diagonal terms of the density matrix. Another explanation would be that volume effects and spatial distribution of the beam are not yet included in the model. Further careful experiments are thus necessary at higher pressures to explore and understand the observed disagreements.

REFERENCES

1. Seideman T, Hamilton E. *Adv. At. Mol. Opt. Phys.* 2006; **52**: 289.
2. Stapelfeldt H, Seideman T. *Rev. Mod. Phys.* 2003; **75**: 543.
3. Dion CM, Keller A, Atabek O. *Eur. Phys. J. D.* 2001; **14**: 249.
4. Machholm M, Henriksen NE. *Phys. Rev. Lett.* 2001; **87**: 193001.
5. Sugny D, Keller A, Atabek O, Daems D, Guérin S, Jauslin HR. *Phys. Rev. A* 2004; **69**: 043407.
6. Renard V, Renard M, Rouzée A, Guérin S, Jauslin HR, Lavorel B, Faucher O. *Phys. Rev. Lett.* 2004; **70**: 033420.
7. Lavorel B, Faucher O, Morgen M, Chaux R. *J. Raman Spectrosc.* 2000; **31**: 77.
8. Ramakrishna S, Seideman T. *J. Chem. Phys.* 2006; **124**: 034101.
9. Sugny D, Kontz C, Jauslin HR. *Phys. Rev. A* 2006; **74**: 053411.
10. Ramakrishna S, Seideman T. *Phys. Rev. Lett.* 2005; **95**: 113001.
11. Ramakrishna S, Seideman T. *J. Chem. Phys.* 2005; **122**: 084502.
12. Fanjoux G, Lavorel B, Millot G. *J. Raman Spectrosc.* 1998; **29**: 391.
13. Weiss U. *Quantum Dissipative Systems*. World Scientific: Singapore, 1999.
14. Boulet C, Bouanich J-P, Hartmann J-M, Lavorel B, Deroussiaux A. *J. Chem. Phys.* 1999; **111**: 9315.
15. Rothman LS, Young YDG. *J. Quant. Spectrosc. Radiat. Transf.* 1981; **25**: 505.
16. Lalanne JR, Kielich S, Ducasse A. In *Interaction laser molécule*. Polytechnica 1994.
17. Lavorel B, Tran H, Hertz E, Faucher O, Joubert P, Motzkus M, Buckup T, Lang T, Skenderovi H, Knopp G, Beaud P, Frey HM. *C. R. Phys.* 2004; **5**: 215.
18. Rouzée A, Renard V, Lavorel B, Faucher O. *J. Phys. B* 2005; **38**: 2329.
19. Lavorel B, Millot G, Saint-Loup R, Berger H, Bonamy L, Bonamy J, Robert D. *J. Chem. Phys.* 1990; **93**: 2176.